

Wolfgang Kinzel Georg Reents

Physics by Computer

Programming Physical Problems
Using Mathematica® and C

Translated by Martin Clajus and Beverly Freeland-Clajus

With 88 Figures, 33 Exercises and a CD-ROM
Containing Programs and Graphics Routines for PCs
and Workstations; Mathematica® 3.0 compatible

Springer
Berlin
Heidelberg
New York
Barcelona
Budapest
Hong Kong
London
Milan
Paris
Santa Clara
Singapore



Springer

2. Use the algorithm `step2[u, w]` for the integration, and choose the initial condition $u(x, 0) = -6 \operatorname{sech}^2 x$. Vary dx between 0.1 and 0.2 and determine the stability limit with respect to dt , for a given dx ; i.e., approximately determine the maximum dt allowed as a function of dx . Confirm (4.61) by displaying the result in a log-log plot.

Literature

- Baumann G. (1996) *Mathematica in Theoretical Physics: Selected Examples from Classical Mechanics to Fractals*. TELOS, Santa Clara, CA
 Crandall R.E. (1991) *Mathematica for the Sciences*. Addison-Wesley, Redwood City, CA

4.5 Time-dependent Schrödinger Equation

If a particle moves in a box without friction or any other force, its motion is changed only by reflection off the walls. In one dimension, therefore, it moves back and forth regularly. This classical picture, which is based on the idea of a pointlike mass with precisely defined position and momentum, no longer holds true if the box is microscopically small. Instead, we have to describe the particle by a wave function. In the quantum mechanics course one learns that the stationary states in this case are standing waves. But what happens to an initially localized wave packet that moves towards the walls of the box?

This problem has both analytic and numerical aspects. We will use the expansion in terms of eigenfunctions in order to make statements about symmetries, recurrence times, and other characteristic length and time scales. On the other hand, we want to use the time-dependent Schrödinger equation to demonstrate how to solve partial differential equations numerically by using an implicit method. This involves inverting a tridiagonal matrix, for which there is a fast numerical method. Additionally, care has to be taken when discretizing the time evolution of the quantum-mechanical state that the normalization of the wave function does not change with time.

We will see that the seemingly simple and well-understood textbook example exhibits a surprisingly complex behavior. The wave packet disperses, and wild interference patterns arise from which smooth wave packets suddenly reemerge. Finally, the entire process repeats periodically with time. The cover of this book shows what complexity and beauty can arise from elementary quantum mechanics.

Physics

Let $\psi(x, t)$ be the complex-valued wave function of a particle with mass m which moves in one dimension in a potential $\tilde{V}(x)$. Then $|\psi(x, t)|^2 dx$ is the

probability of finding the particle in the interval $[x, x + dx]$ at time t . The time dependence of $\psi(x, t)$ is described by the Schrödinger equation in its coordinate representation:

$$i\hbar \frac{\partial \psi}{\partial t} = -\frac{\hbar^2}{2m} \frac{\partial^2 \psi}{\partial x^2} + \tilde{V}(x) \psi. \quad (4.62)$$

In order to put this equation into a dimensionless form, we normalize the time by t_0 and the position by x_0 :

$$i \frac{\hbar}{t_0} \frac{\partial \psi}{\partial (t/t_0)} = -\frac{\hbar^2}{2m x_0^2} \frac{\partial^2 \psi}{\partial (x/x_0)^2} + \tilde{V}(x) \psi. \quad (4.63)$$

Now we choose t_0 and x_0 such that the following equation holds:

$$\hbar t_0 = 2m x_0^2. \quad (4.64)$$

Now if we set $\tilde{V}(x)t_0/\hbar = V(x/x_0)$ and express position and time in units of x_0 and t_0 , we obtain the dimensionless equation

$$i \frac{\partial \psi}{\partial t} = H \psi = \left[-\frac{\partial^2}{\partial x^2} + V(x) \right] \psi. \quad (4.65)$$

H is the normalized Hamiltonian of the particle. There are two ways to numerically solve this equation. First, we can calculate the eigenstates and eigenvalues of the stationary equation $H\psi = E\psi$, expand $\psi(x, 0)$ in terms of these states, and then specify a series representation for $\psi(x, t)$. Second, we can directly integrate the time-dependent equation as shown in the previous section. The second method can even be used for problems for which the first one fails, which is why we want to describe that method in the algorithm section. If, on the other hand, the eigenstates are known, one can use the analytic ansatz to directly derive at least some properties of the wave function $\psi(x, t)$.

We want to study a particle in a box with infinitely high walls. As symmetry considerations will play a significant role in what follows, we position the coordinate system in such a way that this symmetry can be expressed easily. With these considerations, the potential $V(x)$ takes the form

$$V(x) = \begin{cases} 0 & \text{for } -\frac{1}{2} \leq x \leq \frac{1}{2}, \\ \infty & \text{otherwise.} \end{cases} \quad (4.66)$$

Here, the coordinate x is expressed in units of the box's width a , and the energy E in units of $\hbar^2/2ma^2$. The energies E_n of the stationary states $\psi_n(x)$ are known from the quantum mechanics course:

$$E_n = n^2 \pi^2, \quad \text{where } n = 1, 2, 3, \dots, \\ \psi_n(x) = \begin{cases} \sqrt{2} \cos(n\pi x) & \text{for } n \text{ odd} \\ \sqrt{2} \sin(n\pi x) & \text{for } n \text{ even} \end{cases}, \quad -\frac{1}{2} \leq x \leq \frac{1}{2}. \quad (4.67)$$

These states are standing waves whose magnitude does not change as a function of time. The particle's mean position in these states, $\langle x \rangle = 0$, does not change with time either.

We now want to study a wave packet $\psi(x, t)$ that moves back and forth within the box. The function $\psi(x, 0)$ can be expanded in terms of eigenstates, so for $\psi(x, t)$ we obtain

$$\begin{aligned} \psi(x, t) &= \sum_{m=1}^{\infty} \hat{c}_{2m-1} \exp \left[i\pi^2 (2m-1)^2 t \right] \cos \left[(2m-1)\pi x \right] \\ &\quad + \sum_{m=1}^{\infty} \hat{c}_{2m} \exp \left[-i\pi^2 (2m)^2 t \right] \sin \left(2m\pi x \right) \end{aligned} \quad (4.68)$$

$$= \psi_e(x, t) + \psi_o(x, t) \quad (4.69)$$

with expansion coefficients $\{\hat{c}_n\}$. Owing to the symmetry of the basis functions, this expansion yields at the same time the decomposition of $\psi(x, t)$ into its even (ψ_e) and odd (ψ_o) parts.

Thus the general solution of the Schrödinger equation is an infinite superposition of standing waves with the phase factor of each wave changing at a different rate. This gives rise to complex interference patterns that can change very quickly with time (see the results section below). The states in the box have one distinctive feature, however, that is related to the structure of the energies E_n . Each frequency $\omega_n = n^2\pi^2$ is an integer multiple of the fundamental frequency $\omega_1 = \pi^2$. From this it follows that $\psi(x, t)$ is a periodic function of time, with period $T = 2\pi/\omega_1 = 2/\pi$. After the time $t = T$ has elapsed, the wild interference patterns vanish and the wave packet $\psi(x, t)$ entirely returns to its initial state $\psi(x, 0)$.

We will see in the results section that simple patterns emerge even at certain earlier times. For example, after a time $t = T/2$ the initial distribution reemerges, reflected about the center of the box, moving exactly in the opposite direction. We want to present a brief analytic proof of this. At the time $t = T/2 = 1/\pi$, all phase factors in $\psi_e(x, t)$ give the factor -1 , since $\exp(-i\pi(2m-1)^2) = -1$, whereas the exponentials in $\psi_o(x, t)$ all have the value 1 for $t = 1/\pi$. Consequently, we obtain

$$\begin{aligned} \psi\left(x, \frac{T}{2}\right) &= -\psi_e(x, 0) + \psi_o(x, 0) \\ &= -\psi_e(-x, 0) - \psi_o(-x, 0) = -\psi(-x, 0). \end{aligned} \quad (4.70)$$

Thus after the time $T/2$ the initial probability distribution $|\psi(x, 0)|^2$ is back, but it is reflected about the center of the box, $x = 0$. That the wave moves in the opposite direction can best be seen from the current density,

$$j(x, t) = i \left[\psi(x, t) \frac{\partial \psi^*}{\partial x}(x, t) - \psi^*(x, t) \frac{\partial \psi}{\partial x}(x, t) \right]. \quad (4.71)$$

If we insert the result from (4.70) here, we immediately get

$$j\left(x, \frac{T}{2}\right) = -j(-x, 0). \quad (4.72)$$

We have shown that at the times $T/2$ and T the original form reemerges from the complex interference patterns. The results section shows, however, that

simple waves arise even earlier. For example, at $T/4$ we get two wave packets which move towards one another and interfere with each other later. This is a consequence of the initial condition we have chosen,

$$\psi(x, 0) = e^{ikx} \exp \left[-\frac{1}{2\sigma^2} \left(x + \frac{1}{4} \right)^2 \right]. \quad (4.73)$$

The function ψ is a Gaussian of width σ , which is concentrated near $x = -1/4$, multiplied by $\exp(ikx)$. Owing to this factor, the particle has an initial velocity

$$\langle v \rangle_0 = \frac{\langle \psi_{t=0} | (p/m) | \psi_{t=0} \rangle}{\|\psi\|^2} = \frac{\hbar k}{m} = 2k. \quad (4.74)$$

The width σ has to be sufficiently small that the boundary condition $\psi(\pm 1/2, 0) = 0$ can be regarded as fulfilled to sufficient precision. For the numerical simulation we use $\sigma = 0.05$, i.e., $|\psi(\pm 1/2, 0)| \leq \exp(-12.5) \lesssim 4 \cdot 10^{-6}$ as compared to $|\psi(-1/4, 0)| = 1$.

We insert $t = T/4 = 1/(2\pi)$ into (4.68). Now the phase factors yield $\exp[-i\pi^2(2m-1)^2/(2\pi)] = -i$ and $\exp[-i\pi^2(2m)^2/(2\pi)] = 1$ respectively, and we obtain

$$\psi\left(x, \frac{T}{4}\right) = -i\psi_e(x, 0) + \psi_o(x, 0). \quad (4.75)$$

Consequently, the norm of the wave function for $t = T/4$ is

$$\begin{aligned} \left| \psi\left(x, \frac{T}{4}\right) \right|^2 &= |\psi_e(x, 0)|^2 + |\psi_o(x, 0)|^2 \\ &\quad + i[\psi_e^*(x, 0)\psi_o(x, 0) - \psi_e(x, 0)\psi_o^*(x, 0)]. \end{aligned} \quad (4.76)$$

The last term of this equation, which can be written as $2 \operatorname{Im}(\psi_e(x, 0)\psi_o^*(x, 0))$, is negligibly small. A simple calculation using (4.73) yields

$$2 \operatorname{Im}[\psi_e(x, 0)\psi_o^*(x, 0)] = -2 \exp \left[-\frac{1}{2\sigma^2} \left(\frac{1}{8} + 2x^2 \right) \right] \cos kx \sin kx, \quad (4.77)$$

i.e., a term which for $\sigma = 0.05$ is of the order $\exp(-25)$. The remainder can be expressed by $\psi(\pm x, 0)$ in the following way:

$$\begin{aligned} |\psi_e(x, 0)|^2 + |\psi_o(x, 0)|^2 &= \frac{1}{2} [|\psi_e(x, 0) + \psi_o(x, 0)|^2 + |\psi_e(x, 0) - \psi_o(x, 0)|^2] \\ &= \frac{1}{2} [|\psi_e(x, 0) + \psi_o(x, 0)|^2 + |\psi_e(-x, 0) + \psi_o(-x, 0)|^2] \\ &= \frac{1}{2} [|\psi(x, 0)|^2 + |\psi(-x, 0)|^2]. \end{aligned}$$

In summary we obtain

$$\left| \psi\left(x, \frac{T}{4}\right) \right|^2 \cong \frac{1}{2} [|\psi(x, 0)|^2 + |\psi(-x, 0)|^2], \quad (4.78)$$

i.e., just a symmetrized version of the initial distribution. The corresponding calculation for the current density yields

$$j(x, \frac{T}{4}) \cong \frac{1}{2} j(x, 0) - \frac{1}{2} j(-x, 0), \tag{4.79}$$

which shows that the two wave packets (4.78) move towards each other.

At even shorter times, waves with a simple structure arise as well. If we set $t = T p/q$ with integers p and q which are relatively prime, the phase $\exp(-2\pi i n^2 p/q)$ can take at most q different values. Therefore, according to (4.68), $\psi(x, t)$ is a superposition of q waves, each of which is an infinite partial sum out of that same expansion for $\psi(x, 0)$. If we assume that each partial wave is a smooth function, then their superposition is smooth as well and $\psi(x, t)$ exhibits a simple structure at those times. This is precisely what we will observe when we do the numerical integration.

With this we conclude the analytic considerations and turn our attention to the description of the numerical integration of the time-dependent Schrödinger equation.

Algorithm

First, $\psi(x, t)$ is discretized:

$$\psi_n^j = \psi(jdx, n dt). \tag{4.80}$$

Here, j and n are integers, and dx and dt are the step sizes of the space and time coordinates. As before, we write the second derivative as

$$\frac{\partial^2 \psi}{\partial x^2} \rightarrow \frac{1}{(dx)^2} (\psi_n^{j+1} - 2\psi_n^j + \psi_n^{j-1}) \tag{4.81}$$

with an error of the order $\mathcal{O}(dx^2)$. Now we can discretize the time derivative, analogously to the solitons from the previous section. That algorithm, however, does not conserve the overall probability $\int |\psi(x, t)|^2 dx = 1$, which is not allowed to change with time. It is indeed possible to find a discrete approximation of the partial differential equation that conserves the overall probability. To this end, the discretized time evolution operator must be chosen to be unitary.

The solution of the Schrödinger equation (4.65) can also be written in the form

$$\psi(x, t + dt) = e^{-iHdt} \psi(x, t). \tag{4.82}$$

The approximation

$$e^{-iHdt} \simeq (1 - iHdt) + \mathcal{O}(dt^2), \tag{4.83}$$

which corresponds to the simple Euler step, is no longer unitary. On the other hand, with

$$\begin{aligned} e^{-iHdt} &= \left(e^{iHdt/2} \right)^{-1} e^{-iHdt/2} \\ &\simeq \left(1 + \frac{i}{2} Hdt \right)^{-1} \left(1 - \frac{i}{2} Hdt \right) + \mathcal{O}(dt^3) \end{aligned} \tag{4.84}$$

one obtains a unitary operator for the discrete time evolution:

$$\psi_{n+1}^j = \left(1 + \frac{i}{2} Hdt \right)^{-1} \left(1 - \frac{i}{2} Hdt \right) \psi_n^j. \tag{4.85}$$

Now the overall probability $\sum_j |\psi_n^j|^2$ remains constant as a function of time n . The inverse operator can be moved to the left side of the equation just as well,

$$\left(1 + \frac{i}{2} Hdt \right) \psi_{n+1}^j = \left(1 - \frac{i}{2} Hdt \right) \psi_n^j. \tag{4.86}$$

In this form, the difference equation becomes an implicit equation; this means that the wave function in the next time step is determined by a system of equations that has to be solved first. The corresponding algorithm takes more processing time, but it leads to a more stable numerical procedure in almost all cases. If we now insert the particular form of the Hamiltonian, we obtain

$$(H\psi)_n^j = -\frac{1}{(dx)^2} (\psi_n^{j+1} - 2\psi_n^j + \psi_n^{j-1}) + V^j \psi_n^j. \tag{4.87}$$

With this, (4.86) yields

$$\begin{aligned} \psi_{n+1}^{j+1} + \left(i \frac{2(dx)^2}{dt} - (dx)^2 V^j - 2 \right) \psi_{n+1}^j + \psi_{n+1}^{j-1} = \\ -\psi_n^{j+1} + \left(i \frac{2(dx)^2}{dt} + (dx)^2 V^j + 2 \right) \psi_n^j - \psi_n^{j-1} = \Omega_n^j. \end{aligned} \tag{4.88}$$

We have abbreviated the second line, which only contains terms referring to the time step n , by Ω_n^j . This equation has the form

$$T\psi_{n+1} = \Omega_n, \tag{4.89}$$

with a tridiagonal matrix T . Therefore we have to solve a system of linear equations. In the case of tridiagonal matrices, there is a special method for this. We use the ansatz

$$\psi_{n+1}^{j+1} = \alpha^j \psi_{n+1}^j + b_n^j. \tag{4.90}$$

If we insert this in (4.88), we find

$$\psi_{n+1}^j = \left[2 + (dx)^2 V^j - i \frac{2(dx)^2}{dt} - \alpha^j \right]^{-1} \left[\psi_{n+1}^{j-1} + b_n^j - \Omega_n^j \right]. \tag{4.91}$$

Comparison with (4.90) yields equations for α^{j-1} and b_n^{j-1} , which we can solve for α^j and b_n^j . The result is

$$a^j = 2 + (dx)^2 V^j - i \frac{2(dx)^2}{dt} - \frac{1}{a^{j-1}}, \quad (4.92)$$

$$b_n^j = \Omega_n^j + \frac{b_n^{j-1}}{a^{j-1}}.$$

As required by the ansatz (4.90), a^j is independent of n , whereas b_n^j is calculated from the wave function ψ_n^j . To solve these equations, we need the initial state ψ_0^j and boundary conditions. Since we want to confine the particle in a box with infinitely high walls, ψ has to vanish at the boundary,

$$\psi_n^0 = 0 \quad \text{and} \quad \psi_n^j = 0, \quad (4.93)$$

where we have redefined the boundary as $x = 0$ and $x = 1$, as this is easier to program. The number of grid points, J , is thus fixed at $J = 1 + 1/dx$. At $j = 1$, (4.88) becomes

$$\psi_{n+1}^2 + \left(i \frac{2(dx)^2}{dt} - (dx)^2 V^1 - 2 \right) \psi_{n+1}^1 = \Omega_n^1. \quad (4.94)$$

A comparison with (4.90) gives

$$a^1 = 2 + (dx)^2 V^1 - i \frac{2(dx)^2}{dt}, \quad b_n^1 = \Omega_n^1. \quad (4.95)$$

From these initial values, all a^j can be calculated using (4.92), as can all b_n^j after each time step. The wave function is then calculated from (4.90) by inverse iteration:

$$\psi_{n+1}^j = \frac{\psi_{n+1}^{j+1} - b_n^j}{a^j}. \quad (4.96)$$

Since the boundary value on the right, $\psi_{n+1}^j = 0$, is fixed, this allows the calculation of the entire vector ψ_{n+1}^j at the time step $n + 1$. All results are now combined into one algorithm:

1. Choose an initial state ψ_0^j and use it to calculate Ω_0^j according to (4.88).
2. Calculate the vector a^j from the initial value given in (4.95) and the recursion formula (4.92).
3. For all positions j , calculate the variable b_n^j , using the initial value from (4.95) and the recursion formula (4.92).
4. Use (4.96) to calculate the values of the wave function ψ_{n+1}^j for the next time step, using the initial value $\psi_{n+1}^j = 0$. This also yields Ω_{n+1}^j according to (4.88).
5. Repeat steps 3 and 4 for $n = 0, 1, 2, \dots$

As mentioned before, we define the initial state as a Gaussian wave packet that moves with a mean momentum k :

$$\psi(x, 0) = e^{ikx} \exp \left[-\frac{(x - x_0)^2}{2\sigma^2} \right]. \quad (4.97)$$

The equations above are easily formulated in any programming language. In doing so, it has to be noted, however, that the quantities $\{\psi_n^j\}$, $\{a^j\}$, and $\{b_n^j\}$ are complex numbers. Whereas *Mathematica*, as well as other languages like Fortran, can deal with those numbers directly, in C one has either to include the appropriate routines, e.g., from *Numerical Recipes*, or to define a structure with a real and imaginary part oneself:

```
typedef struct{double real, imag; } complex;
```

In this case, one also has to write multiplication and division routines oneself. For example, the well-known multiplication and division formulae for complex numbers $a = \text{Re}a + i\text{Im}a$ and $b = \text{Re}b + i\text{Im}b$,

$$a \cdot b = \text{Re}a\text{Re}b - \text{Im}a\text{Im}b + i(\text{Im}a\text{Re}b + \text{Re}a\text{Im}b), \quad (4.98)$$

$$\frac{a}{b} = \frac{\text{Re}a\text{Re}b + \text{Im}a\text{Im}b + i(\text{Im}a\text{Re}b - \text{Re}a\text{Im}b)}{(\text{Re}b)^2 + (\text{Im}b)^2} \quad (4.99)$$

can be found in the function `calculate_b` which performs the iteration of (4.92)

```
void calculate_b(complex *b, complex *omega, complex *a)
{
  int j ; double a2;
  b[1].real=omega[1].real;
  b[1].imag*omega[1].imag;
  for (j=2;j<J;j++)
  {a2=a[j-1].real*a[j-1].real+a[j-1].imag*a[j-1].imag;
    b[j].real=omega[j].real+
    (b[j-1].real*a[j-1].real+b[j-1].imag*a[j-1].imag)/a2;
    b[j].imag=omega[j].imag+
    (b[j-1].imag*a[j-1].real-b[j-1].imag*a[j-1].imag)/a2;
  }
}
```

All other steps of the algorithm above can be programmed just as easily. We refer the reader to the source code on the enclosed CD-ROM.

To numerically integrate the Schrödinger equation we have chosen the interval $[0, 1]$ for the box, because, among other things, this makes it easier to convert the x -coordinate to the positive screen coordinates. The eigenfunction expansion that corresponds to (4.68) is then given by:

$$\psi(x, t) = \sum_{n=1}^{\infty} c_n \exp(-in^2\pi^2 t) \sin(n\pi x), \quad (4.100)$$

$$c_n = 2 \int_0^1 \sin(n\pi x) \psi(x, 0) dx. \quad (4.101)$$

The initial state in our simulation is the Gaussian wave packet (4.97) with a width $\sigma = 0.05$ and the mean momentum $k = 40$ which is centered at $x_0 = 0.25$. As we have already seen, the wave has to return to its initial state

after the time $T = 2/\pi \approx 0.6366$. This provides a test of the accuracy with which we have integrated the Schrödinger equation.

Of course, T is also the largest time scale that is relevant for this problem. In addition, though, there are three other characteristic time scales that play a role in this case. First, there is the time it takes the particle to traverse the box once, given its momentum. For $k = 40$, we obtain $t_1 = 1/80 = 0.0125$ from (4.74). Next, we have to take into account the dispersion of the wave packet, which is a typical effect of quantum mechanics. A free Gaussian distribution with an initial width σ will have the width $\sigma\sqrt{1 + \hbar^2 t^2/(4m^2\sigma^4)}$ at time t . By asking when this width will agree with the size of the box, we obtain the time scale $t_2 \approx 1/20 = 0.05$.

Finally, the fourth time scale, which also gives us a handle on selecting the step sizes dx and dt , is determined by the highest relevant phase velocity, for whose determination we make use of (4.100) and (4.101). If we express the sine in these equations by an exponential function, the individual terms in the sum (4.100) take the form

$$c_n \exp[-in\pi(n\pi t \pm x)], \tag{4.102}$$

so the phase velocity v_n^{ph} for this partial wave has the value

$$v_n^{\text{ph}} = \pm n\pi. \tag{4.103}$$

To estimate up to which n the coefficients c_n give significant contributions, we note that the Fourier transform of a Gaussian is a Gaussian again, but with the reciprocal width. The factor $\exp(ikx)$ turns into a shift by the distance k in Fourier space. From this, we can derive the n -dependence of c_n

$$|c_n| \propto \exp\left[-\frac{1}{2}\sigma^2(n\pi - k)^2\right]. \tag{4.104}$$

On the screen, we can only display those amplitudes which amount to at least 1/1000 of the maximum amplitude. This leads us to the estimate

$$\frac{1}{2}\sigma^2(n\pi - k)^2 \leq \ln(1000) \Rightarrow n_{\text{max}} \approx 35, \quad v_{\text{max}}^{\text{ph}} \approx 100. \tag{4.105}$$

With the requirement that the shortest arc among those sines be covered by about 20 to 30 steps, this consideration leads to

$$dx \lesssim 10^{-3} \quad \text{and} \quad dt \lesssim 10^{-5}, \tag{4.106}$$

since dt should not be larger than $dx/v_{\text{max}}^{\text{ph}}$ in any case.

If one also wants to take into account the global aspect that the integration should be correct for at least the duration of a period, the step size dt can be determined more accurately by the following consideration. While the algorithm we use guarantees that the norm of the wave function is conserved, it still represents an approximation. For while the exact time evolution of the eigenmode $\psi_n(x)$ after ℓ steps is given by the factor $\exp(-in^2\pi^2\ell dt)$, the numerical calculation according to (4.85) yields

$$\left(\frac{1 - in^2\pi^2 dt/2}{1 + in^2\pi^2 dt/2}\right)^\ell = e^{i\ell d\varphi}, \quad \text{where } d\varphi = 2 \arctan\left(\frac{n^2\pi^2 dt}{2}\right). \tag{4.107}$$

For the absolute value of the difference between these two expressions, the Taylor expansion of $d\varphi$ gives the result

$$\Delta \approx \frac{1}{12}\ell (dtn^2\pi^2)^3. \tag{4.108}$$

If we require that $\Delta < 1/2$ for $\ell = T/dt$ and $n = n_{\text{max}}$, we obtain a step $dt \lesssim 2 \cdot 10^{-6}$. It turns out that for $dx = 10^{-3}$ and $dt = 5 \cdot 10^{-6}$ our algorithm produces reasonable results which do, however, exhibit deviations from the exact time evolution as the integration time increases.

Results

Initially, the wave does not yet notice the box. It moves to the right and disperses in the process. As soon as part of the wave is reflected off the wall, though, it interferes with the part that is still coming in, forming a wave pattern (Fig. 4.13, left). In the right-hand part of the figure one can see that after just a short time ($t = T/40$) an irregular interference pattern has formed that spans the entire box. This pattern is typical for almost all times.

Suddenly, though, regular shapes arise from the seemingly chaotic movements, as can be seen in Figs. 4.14 and 4.15 for the times $T/12$, $T/4$, $T/3$, and $T/2$. As shown before, two wave packets form at $t = T/4$, which move towards and then interfere with one another (Fig. 4.14, right), and at $t = T/2$ the original wave suddenly reemerges, reflected about the center of the box and moving to the left (Fig. 4.15, right). These simple patterns, however, quickly disperse and interfere again to generate wild movements.

In Fig. 4.16, the individual pictures for different times are combined into a mountain range rising above the x - t plane. The spatial coordinate is displayed horizontally from right to left and time from back to front. At the back, one can see how the initial state first moves to the left, dispersing in the

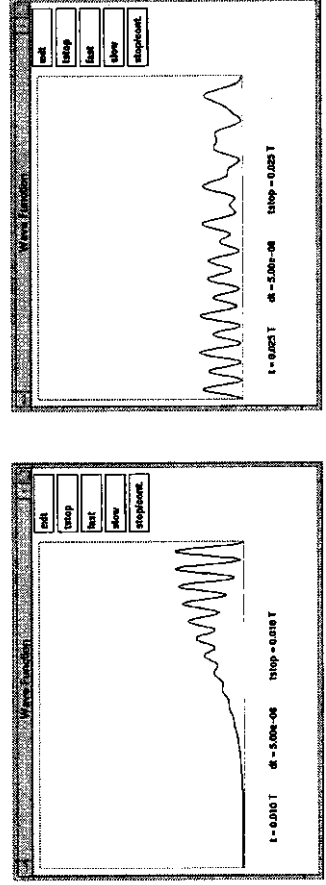


Fig. 4.13. The wave packet $|\psi(x, t)|^2$ shortly after the first impact on the wall ($t = T/100$, left) and a typical interference pattern $|\psi(x, t)|^2$ for $t = T/40$ (right)

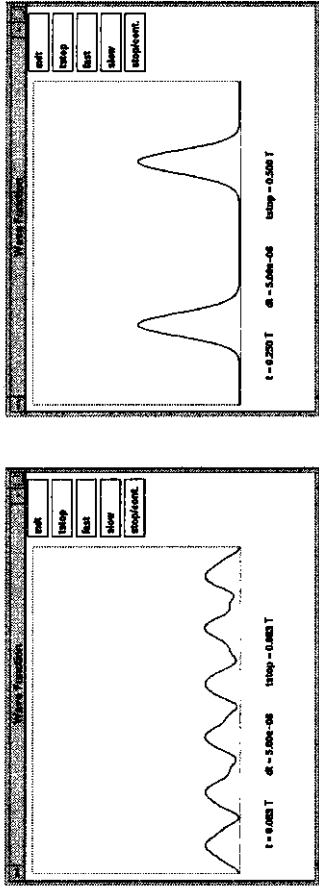


Fig. 4.14. The wave packet $|\psi(x, t)|^2$ at times $t = T/12$ (left) and $t = T/4$ (right)

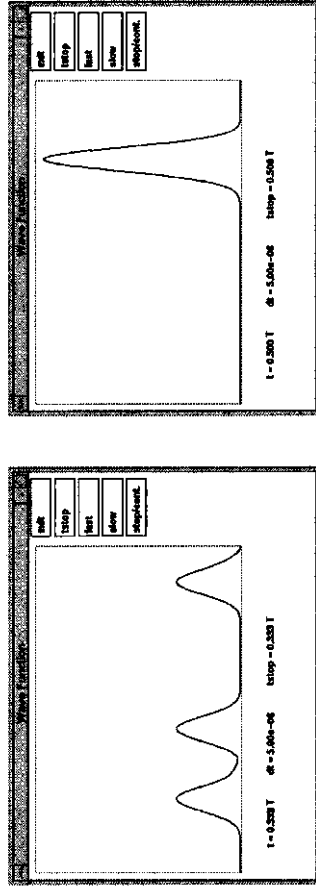


Fig. 4.15. The wave packet $|\psi(x, t)|^2$ at times $t = T/3$ (left) and $t = T/2$ (right)

process, and then is reflected off the wall. In the foreground, the probability distribution just before the time $T/6$ can be seen: a smooth wave with three peaks. In between, a fascinating hilly landscape of unexpected variety and regularity arises. In particular the valleys, which spread out in star shapes, did not attract our attention while studying the wave directly on the screen. So far, we have not been able to calculate these valleys analytically.

Finally, Fig. 4.17 shows both the initial distribution $|\psi(x, 0)|^2$ (dotted) and the numerically integrated wave packet after a full period T . If we wanted to eliminate the obvious discrepancy between the numerical solution and the exact time evolution, we would have to refine the discretization of the spatial coordinate even more. This is because so far we have used the energy values $E_\nu = \nu^2 \pi^2$ of the exact Hamiltonian H in our considerations regarding the duration of a period, whereas for the numerical integration the matrix version of H , (4.87) with $V^j = 0$, is relevant. The eigenvalues E_ν^d of this operator and the corresponding eigenvectors ϕ_ν^d , which, of course, are subject to the boundary conditions (4.93), are known as well, however:

$$\phi_\nu^d = \sin(\nu\pi j dx), \quad E_\nu^d = \frac{4}{(dx)^2} \sin^2\left(\frac{\nu\pi}{2}\right). \quad (4.109)$$

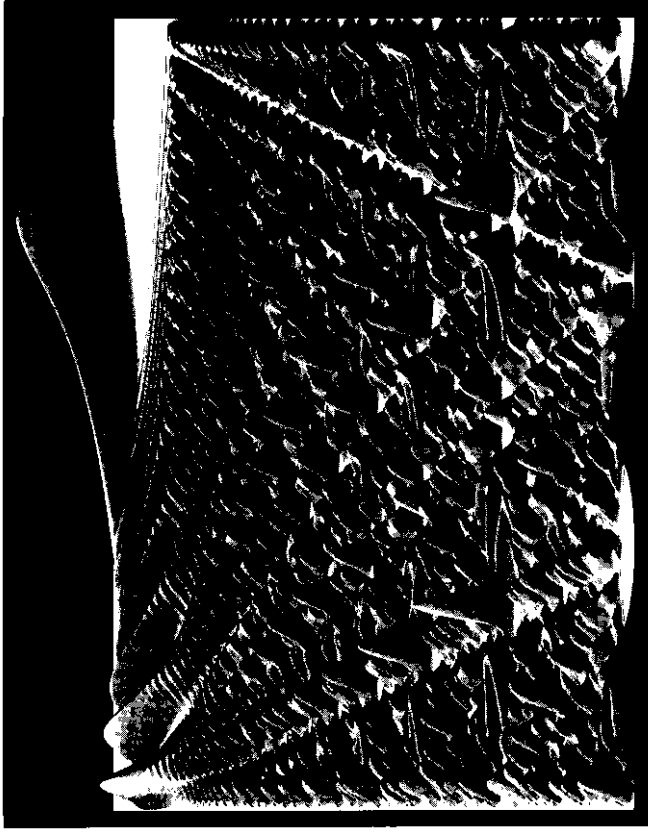


Fig. 4.16. Space-time diagram of the probability of presence of a quantum particle in a square-well potential

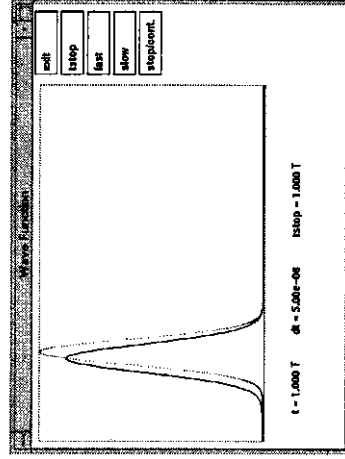


Fig. 4.17. The initial distribution $|\psi(x, 0)|^2$ (dotted) and the numerically integrated wave packet $|\psi(x, T)|^2$ after the full period T (solid curve)

From the equation above and the expansion of E_v^d for $dx \ll 1$,

$$E_v^d \simeq v^2 \pi^2 - \frac{1}{12} v^4 \pi^4 (dx)^2, \quad (4.110)$$

we conclude first that the frequencies no longer are integer multiples of a fundamental frequency, and second that all of them are smaller than the E_v previously considered. This explains both the broadening and the time delay of the wave packet in Fig. 4.17. By taking the modified energy values E_v^d according to (4.109) into account in (4.107) one obtains $dx \lesssim 10^{-4}$ and $dt \lesssim 10^{-6}$ if one does not want this correction to be noticeable after one period.

Exercises

- Use the integration routine described in this section to calculate and display the mean values $\langle x \rangle$, $\langle p \rangle$, and their uncertainties Δx , Δp as a function of time.
- The program code above is easily modified to demonstrate the tunnel effect. Change the potential inside the box by putting a Gaussian barrier of the form

$$V_0 \exp \left[-\frac{(x - 1/2)^2}{2d^2} \right]$$

in its center. Try finding a numerical criterion for the tunneling time t_T . For example, the probability w_n of finding the particle on the right-hand side of the barrier at the time $t_n = n\Delta t$ is given by

$$w_n = \frac{\sum_{j=J/2}^J |\psi_n^j|^2}{\sum_{j=1}^J |\psi_0^j|^2}.$$

Numerically determine the dependence of the tunneling time V_0 on the width d of the barrier.

Literature

Dahmen H.D., Brandt S. (1994) Quantum Mechanics on the Personal Computer. Springer, Berlin, Heidelberg, New York
 Koonin S.E., Meredith D.C. (1990) Computational Physics, Fortran Version. Addison-Wesley, Reading, MA

5. Monte Carlo Simulations

Monte Carlo \rightarrow casino \rightarrow roulette \rightarrow random numbers: This is the chain of associations which gave an important method of computer simulation its name. With the help of random numbers, one can use the computer to simulate, for example, the motion of an interacting many-body system in a heat reservoir. As in the real experiment the temperature and other parameters can be varied. The materials being modeled can be heated up or cooled down, and at sufficiently low temperatures one can observe how gases liquefy, how atoms in a magnetic material get aligned, or how metals lose their electric resistance.

Here we want to use simple examples to study how interesting physics phenomena can be described with the help of random numbers. Some of these models even have universal properties: The values of the critical exponents that describe the singularities at phase transitions are the same for many different models and are even measured in real materials. Therefore computer simulation is a particularly important tool for understanding the cooperative properties of interacting particles.

5.1 Random Numbers

A computer cannot generate random numbers. It works according to a well-defined program, i.e., according to rules which are applied to input data and generate output data. Therefore a computer acts like a deterministic function that leaves no room for chance. Still, there are algorithms that generate "pseudo-random" numbers. In many statistical tests, such a sequence of numbers leads to results similar to those we would get from random numbers that fulfill the mathematical definition of "randomness." We want to briefly introduce such algorithms here.

Algorithm and Results

In a computer, numbers are represented by a sequence of bits (0 or 1). If, for example, 32 bits per number are available, a maximum of 2^{32} different numbers can be represented with these bits. Consequently, a function f acting on these numbers,